Maritime traffic surveillance with SENTINEL-1 high resolution images

MARIA C. PROENÇA, JORGE M. MARQUES
Physics Department
University of Lisbon
Estrada Paço do Lumiar 22, 1649-038 Lisboa
PORTUGAL
mcproenca@fc.ul.pt http://www.fc.ul.pt

Abstract: - Automatic ship detection in synthetic aperture radar (SAR) images is a promising subject for maritime surveillance that exploits the characteristics inherent to SAR technology. Since the radars are active devices that do not depend on sunlight and use wavelengths with high atmospheric penetration, the acquisition of images day and night and in virtually all weather conditions becomes possible.

Sentinel-1A is the first of a constellation of two European Synthetic Aperture Radar satellites, and it is operational since 3 October 2014. The data is provided free of charges by the European Space Agency (ESA) and the European Commission within the Copernicus Program. The data set used to implement and test this algorithm consists in 32 images of the same area, near the port of Singapore, acquired between October 2014 and January 2017. This is a harbor known by its intense commercial traffic, where there is also high activity of small fishing boats, and a constant presence of large floating platforms, probably involved in drainage and maintenance of the port bathymetry.

The algorithm is based on a wavelet filter variation that can provide a very smooth image, reducing speckle effects and allowing a precise detection of the targets. It can be used in small computers and take seconds to process large areas.

The accuracy of the results makes possible the use of morphological criteria to filter the candidates detected, in addition to the usual radiometric criteria. The quality of the initial detection of targets is compared with the detection achieved with two of the most popular algorithms used in ship detection with similar processing times, SUMO and LM. The concept of false positives does not apply, as all the candidates are (most probably) ships, but of dimensions not relevant in this case study.

Each image has its own land/sea mask, defining the area of interest (AOI) to work, because there are small variations in the field of view of the SAR, as well as in the image itself: a few images include strips of saturated pixels where discrimination is not possible, and this areas are eliminated from the AOI to save processing resources.

This work intends to make available a quick and efficient algorithm implemented in Matlab for SENTINEL-1 images of level 1 with a pixel nearly square of 10 m, directly downloaded from ESA site (https://scihub.copernicus.eu/dhus/#/home), which can be used at any facility with usual informatics support. Visual interpretation was used to validate the results; validation based on ground truth data acquired by VMS/AIS installed in the considered ships and harbor was not in reach for this amount of data and time spanning.

Key-Words: - Automatic maritime surveillance, ship detection, maritime traffic, maritime security.

1 Introduction

Maritime surveillance had a major evolution with the improvement of synthetic aperture radar (SAR) images that can be acquired day and night, on all weather conditions, [1]. Until very recently, those images had a coarse resolution and were characterized by high levels of noise, as the backscatter echo of the irregular sea surface originate strong signals, although with less coherence than those with origin in the vessels [2]. Nowadays, the SAR resolution becomes high enough to detect small ships and the problem of the noisy background can be overcome with algorithms [3], with different degrees of success [2], [4].

Several systems present operational status for automatic ship detection in SAR images, for the majority relying on Constant False Alarm Rate (CFAR), which assumes a difference of intensity levels between the target and its surrounding area [5]. But these systems are not as good as human operators in situations of higher complexity [6], where the human eye can go beyond the image's

intensity characteristics and local contrast, jumping to a contextual and textural analysis at different scales, and using these approaches as a multiresolution tool.

Following the multiresolution cue, another research line uses detection based on the different behavior of the noise and the target (structural information) in the signal provided by wavelet decomposition [7], [8].

Several variants and the obvious combination of both methods were already achieved in ALOS PALSAR and RADARSAT-1 data [9]. The procedure presented here is also a mix, as it includes the use of wavelets to get a set of candidates, followed by a post processing level with morphological and radiometric criteria to select the set of pretended vessels amongst the candidates.

This paper is organized as follows: the present section 1 provides a brief context on ship detection methods, section 2 describes the data set, section 3 details the proposed methodology illustrating each stage with examples, and section 4 contains the evaluation of the results and discussion.

2 Data set

The data set consists in 32 images acquired by the first satellite of SENTINEL-1 mission, a constellation of two satellites that are central to the Copernicus joint initiative of the European Commission (EC) and European Space Agency. The two satellites operate from the same orbit, about 700 km height, separated by 1800 [10], allowing a revisit time of 6 days. Each SENTINEL-1 carries a single C-band synthetic aperture radar instrument operating at a center frequency of 5.405 GHz, which can work in four exclusive modes: interferometric wide swath mode (IW), wave mode (WM), strip map mode (SM) and extra-wide swath mode (EW), with different resolutions and coverages.

The images used were acquired by SENTINEL-1A in interferometric wide swath mode, single polarization VV, and are level 1 High Resolution (HR) Ground Range Detected (GRD) products, that consist in focused SAR data that has been detected, multi-looked and projected to ground range using an Earth ellipsoid model (WGS 84), without phase information [10]. The final product has approximately square pixels of 10 m [11]. Each complete image has dimensions around 25380 x 16840 pixels, with 16 bit depth.

Due to the processing capacity available to implement and test, a representative working area of 801x1431 pixels was extracted from each image in the data set, at the entrance of Johor Strait, west of Sudong Island, Singapore; five images of this area were used to design and implement the algorithm, and the remaining 27 to assess its performance.

The selected area encompasses the entrance of Johor Strait where we can observe large and very large vessels as well as some floating platforms (Fig. 1), and a zone protected by a jetty where there are always a large number of small fishing boats working.

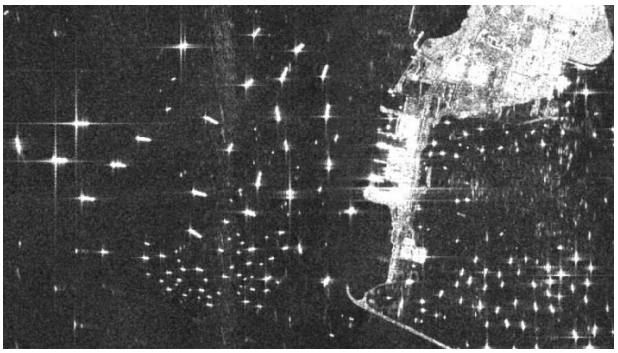

Fig. 1 One Sentinel-1A SAR image of the study area, at the Johor Strait. The goals is to detect the large vessels that offer no reasonable doubt, discarding speckle effects ("stars") and small fishing boats, and discriminate between large and very large ships.

We focus on large vessels (more than 150 m long) and our goal was to detect and count these ships; in the set of objects identified, any discrimination a posteriori becomes possible, for instances to localize and measure very large vessels, or classify and quantify ships by size, or any other user-defined categorization of the elements previously isolated.

We purposely ruled out all the smaller vessels and speckle-enlarged spots in which an outline assessment could be doubtful (Fig. 2).

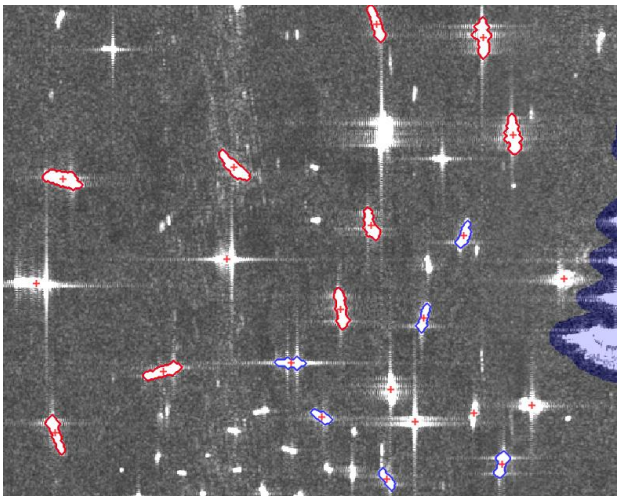

Fig. 2 Although the algorithm detected all the candidates marked with a red cross, we want to focus on large (blue) and very large vessels (red) whose contours could be assessed with sufficient accuracy to measure both length and width.

The first image was acquired in October 2014, and the last at January 2017. The 32 images span 26 months out of the 28, with some in the same months, separated by 24 days.

3 Methodology

The algorithm developed includes an initial filtering stage, followed by segmentation with an image-dependent threshold and a quickly selection of objects in the range of interest.

The pre-processing stage consists in the successive application of a Gaussian filter and a Wiener adaptive noise-removal filtering, based on local statistics estimated in a 7x7 pixel neighborhood. The final filter in the stack is wavelet based filter [12], consisting in wavelets decomposition, followed by reconstruction with sub-band signals suppressed.

This filter does not belong to the Matlab environment used for the implementation: it is a function developed for this effect that uses the basic routines in the wavelet toolbox. Basically, it will decompose the work image with a user defined wavelet until a pre-defined level N, and proceed to the reconstruction of the signal from the approximation of order N, with the sub-band signals suppressed (explicitly equal to zero). In this case, two levels of decomposition/reconstruction are used with a symmetric Daubechies wavelet [13]. The resulting image is normalized and regional minima whose depth is less than 50 are suppressed with an H-minima transform [14].

This initial stage has a strong effect in the background (Fig. 3), smoothing all the characteristic "salt-and-pepper" noise inherent to the SAR technology. The vessels are slightly enlarged, and their outlines have now a sharpen contrast, with contours less prone to the "star" effect of the speckle.

The sequence of filters used improves the overall definition required by a global thresholding procedure, which is the next stage.

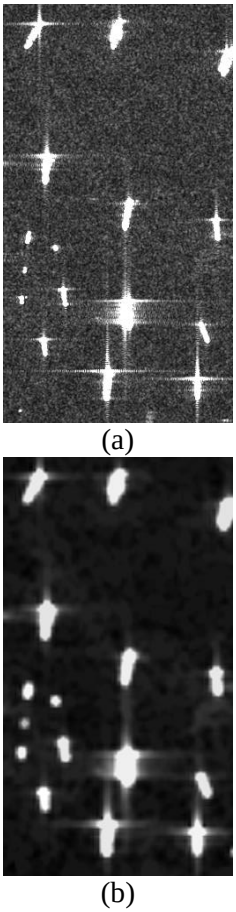

(a) (b)

Fig. 3 Initial and final images in the pre-processing stage, resulting of successive application of three filters (Gaussian, Wiener 2D and wavelets) followed by H-minima transform: a) original image; b) filtered image. Objects are enlarged, the definition of outlines increased, and the "salt-and-pepper noise" in the background is annulated.

To find a threshold to segment the image is now easier; however, not all the images in the data set present exactly the same statistical distribution (compare Fig. 1 and Fig 4, for instances), so the threshold used must be a function of the statistics

reflecting the differences between images, in this case the mean and the standard deviation.

The output image of the pre-processing stage is also used to produce a mask individualized for each image, containing all the land (Fig. 4), which can be complemented to isolate the sea – the working area.

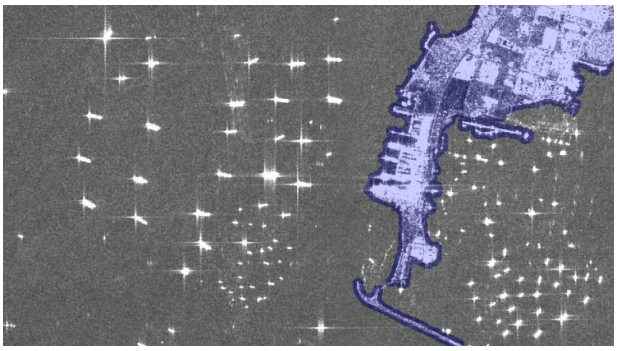

Fig. 4 Land mask projected in the corresponding image.

Applying a threshold at the radiometric level corresponding to the mean of the image less one and a half its standard deviation isolate all size ships, plus land strong signal (Fig. 5); the mask defining the working area eliminates the land.

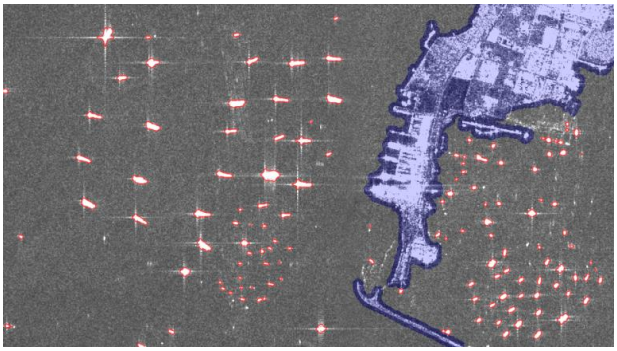

Fig. 5 Contours of all the candidates detected in the working area superposed to the original image.

The last stage of the algorithm consists in candidate selection. After morphological erosion [15] with a disk of radius 2 as structural element, to redefine the outlines more tightly, the first step is a range selection, in order to preserve only the larger ships that are definitely objects of interest (OoI). This is achieved isolating the set of objects in the chosen range – smaller or too large spots where the parallel sides of the vessels cannot be properly identified are discarded (Fig. 6).

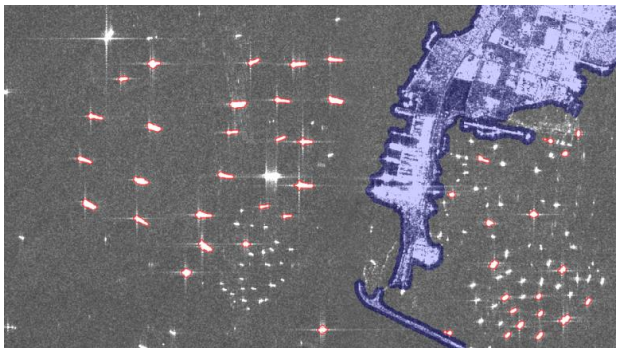

Fig. 6 First selections – smaller and larger objects are selected by range, keeping only candidates with areas between 150 and 700 pixels (compare to Fig. 5).

The next step is a pixel-based evaluation of the original radiometric values for each candidate. The goal is to separate aggregates of small objects, that happens when the ships are very close to each other; five examples in the same image can be seen in Fig. 7 (a). Radiometry based segmentation can solve this issue, leaving darker pixels out of the OoI. The segmentation take place only in the set of pixels belonging to the mask of candidates; the intensity levels are evaluated in the corresponding locations of the original image to decide if the pixel remains in the mask or is turned off. Once the OoI individualized (Fig. 7 (b)), a new application of area-based filter eliminates candidates smaller than the minimum area required and small debris.

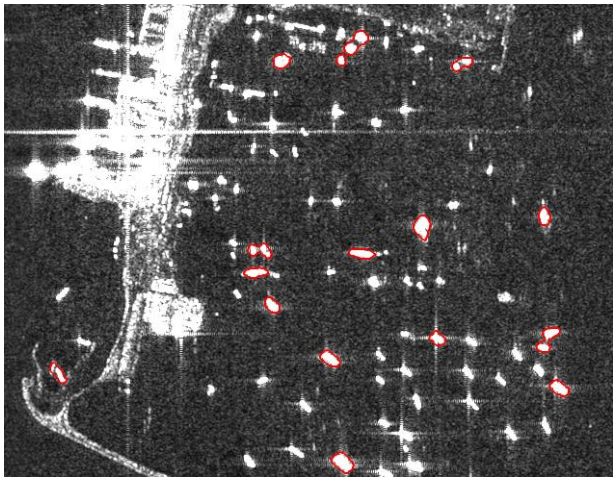

(a)

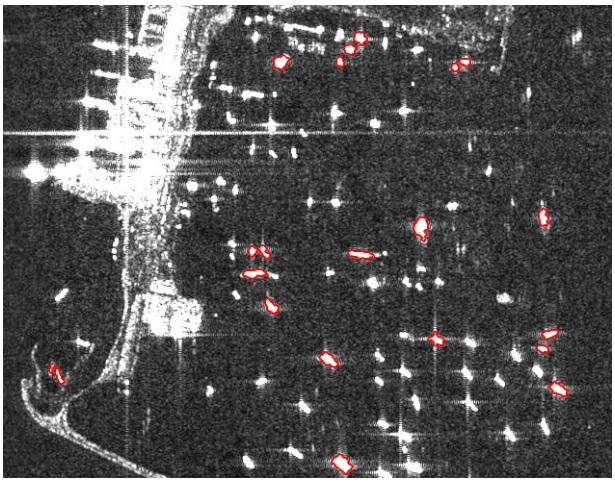

(b)

Fig. 7 Aggregation is solved using the original radiometry: each pixel belonging to a candidate is kept or discarded according to its original intensity; a) example of an image with 5 candidates composed of aggregates; b) the five aggregates separated.

The remaining candidates are filtered based on the features expected to this pattern: form, dimensions, solidity.

The form of a large vessel is always oblong, so its eccentricity should be high. The eccentricity computed for each candidate is that of the ellipse that has the same second-moments; the eccentricity being the ratio of the distance between the foci of the ellipse and its major axis length, a zero eccentricity is actually a circle, and a 1 is a line segment, to which a ship should resemble – a threshold of 0.9 is used (Fig.8).

As the proposed procedure must count ships, some very large candidates must be discarded, because we cannot know if they are two ships side by side or a large floating platform, like the ones used to dredge the estuaries and ensure the navigability for large vessels. Both had been identified in Google Maps images of this area [16].

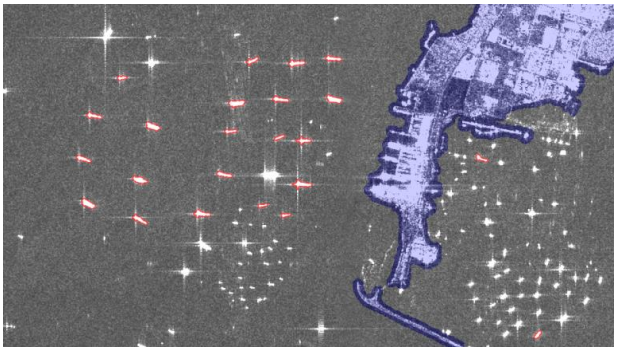

Fig. 8 Filter based in the eccentricity applied to the set of candidates outlined in Fig. 6. Only candidates with eccentricity greater than 0.9 are validated.

So the next step in the candidates' selection is to choose those with a width acceptable for a single ship. The width is computed as the minor axis of the ellipse that encompasses the spot, and can be considered around 15 pixels. The difference in width between some normal vessels and one of those large spots can be observed in Fig. 9.

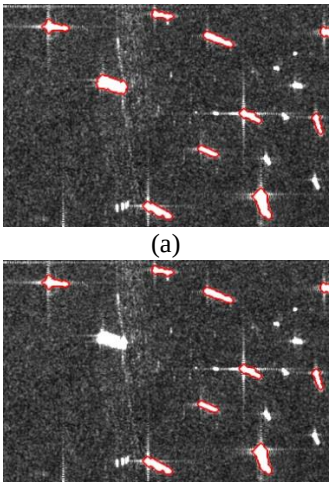

(a)

(b)

Fig. 9 a) A large rectangle included in the set of candidates is discarded (b). The candidates are filtered based on its width, computed has the minor axis of an ellipse encompassing the spot.

The last feature tested is solidity, a figure specifying the proportion of pixels in the convex hull of a spot that also belong to that spot (the convex hull being defined as the smallest convex polygon that contains the region). If it had passed all previous tests, a candidate such as illustrated in Fig. 10 would not satisfy the criteria of solidity.

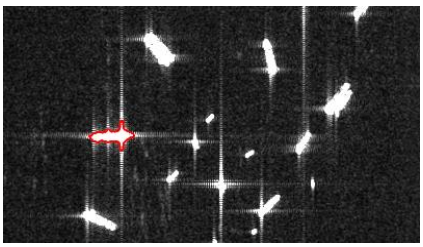

Fig. 10 Example of a candidate with low solidity (inferior to 0.7) that would be eliminate by this criteria.

The candidates that satisfy all the criteria can now be analyzed, for instances, separated by dimensions, orientation, or any other criterion of interest to the end user.

4 Conclusions

The initial detection of this wavelet based (WB) algorithm was compared to two of the most popular algorithms in use that has approximately the same processing time: Search for Unidentified Maritime Objects (SUMO), developed at Joint Research Center and based on template matching [1], and Lockheed Martin (LM), proposed by Lockheed Martin Canada [17], based in a combination of Constant False Alarm Rate (CFAR) detectors with a wavelet transform.

In a workstation with two processors Intel 5160@3GHz, 8GB of RAM, running Windows 7 Enterprise, 64 bits and using the version 2014b of Matlab, the mean processing time for a set of 1900x3930 pixels image samples extracted from the 27 work images was 1.39 second for the wavelet based algorithm proposed, 2.56 second for SUMO algorithm and 21.02 second for LM.

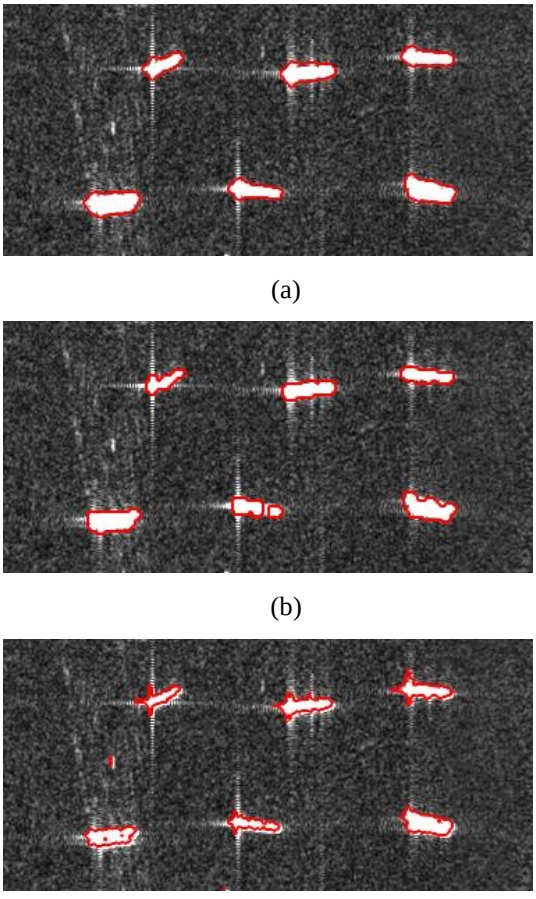

(a)

(b)

(c)

Fig. 11 Detail of the initial detection of targets in three algorithms with a similar processing time: a) this wavelet based algorithm, b) the LM procedure and c) the SUMO algorithm.

The results show that the algorithm presented in this paper has a few small advantages since the initial detection (Fig. 11): i) the contours of the spot corresponding to each possible target are smoother;

ii) there are less broken objects and

iii) less sensibility to speckle.

This differences give a more reliable candidates set and the last post-processing stage, where the candidates are confirmed or refused, is simplified as the contours are very close to the vessels real form.

Using the same mathematical tool that [7] that search for the bursts that eventually correspond to ships in a multiresolution scheme, we use it in the pre-processing stage to be sure that a clear discrimination between the vessels and the noisy background can be achieved automatically.

This algorithm is a complete tool for improving automatic ship detection with SENTINEL-1 images which are free and available to the public in a very short delay after acquisition, that may allow identifying potential targets and enabling major policy decisions, so effective action can be taken – with precise targets located in space and time.

References:

[1] D. J. Crisp, The state-of-the-art in ship detection in synthetic aperture radar imagery, *DSTO Information Sciences Laboratory*, DSTO–RR–0272, 2004.

[2] W. Juan, S. Lijie and Z. Xuelan, Study evolution of ship target detection and recognition in SAR imagery, *Proceedings of the 2009 International Symposium on Information Processing (ISIP'09),* P. R. China, 2009, pp. 147-150.

[3] A. Marino, M. J. Sanjuan-Ferrer, I. Hajnsek, K. Ouchi, Ship detection with spectral analysis of synthetic aperture radar: a comparison of new and well-known algorithms, *Remote Sensing*, Vol. 7, No.5, 2015, pp. 5416-5439.

[4] H. Greidanus, P. Clayton, M. Indregard, G. Staples, N. Suzuki, P. Vachoir, C. Wackerman, T. Tennvassas, J. Mallorqui, N. Kourti, R. Ringrose, H. Melief, Benchmarking operational SAR ship detection, *Proceedings of International Geoscience and Remote Sensing Symposium (IGARSS 2004)*, Vol. 6, 2004, pp. 4215-4218, USA.

[5] T. N. Arnesen and R. B. Olsen, Literature review on vessel detection, FFI/RAPPORT-2004/02619, Norwegian Defence Research Establishment, Kjeller, Norway, 2004.

[6] H. Greidanus and N. Kourti, Findings of the DECLIMS project – detection and classification of marine traffic from space, *Proceedings of SEASAR 2006*, Italy, 2006.
[7] M. Tello, C. López-Martínez, J. Mallorqui, A novel algorithm for ship detection in SAR imagery based on the wavelet transform, *IEEE Geoscience and Remote Sensing Letters*, Vol. 2, No. 2, 2005.
[8] M. Tello, C. López-Martínez, J. Mallorqui, Automatic vessel monitoring with single and multidimensional SAR images in the wavelet domain, *ISPRS Journal of Photogrammetry and Remote Sensing*, Vol. 61(3–4), 2006, pp. 260-278.
[9] F. Meyer and S. Hinz, Automatic ship detection in space-borne SAR imagery, *ISPRS Proceedings*, Hannover, 2009.
[10] https://sentinels.copernicus.eu/documents/247904/685163/Sentinel-1 User_Handbook (accessed 05-04-2017).
[11] https://sentinel.esa.int/documents/247904/349449/S1_SP-1322_1.pdf (accessed 05-04-2017).
[12] S. Mallat, A theory of multiresolution signal decomposition: the wavelet representation, *IEEE Transactions on Pattern Analysis and Machine Intelligence*, Vol. 11, No. 7, 1989, pp. 674 – 693.
[13] I. Daubechies, The wavelet transform, time-frequency localization and signal analysis, *IEEE Transactions on Information Theory*, Vol. 36, No. 5, 1990, pp. 961-1005.
[14] P. Soille, *Morphological image analysis: principles and applications*. Springer-Verlag, pp. 170-171, 1999.
[15] W. K. Pratt, Digital image processing. Third edition, chap. 14, Ed. J. Wiley & Sons, 2001.
[16] https://www.google.pt/maps/place/Sudong+Island/@1.2224565,103.6231072,1978m/data=!3m1!1e3!4m5!3m4!1s0x31da02d055d51961:0x90c04c4cc7de2776!8m2!3d1.207916!4d103.7202285?hl=pt-PT (accessed 12-04-2017).
[17] L. Gagnon, H. Oppenheim and P. Valin, R&D Activities in Airborne SAR Image Processing/Analysis at Lockheed Martin Canada, *Internacional Conf. on Applications of Photonic Technology III*, 1998, pp. 998-1003.